Synthesis, Morphology, and Field-Effect Mobility of Anthradithiophenes

Joyce G. Laquindanum, Howard E. Katz,* and Andrew J. Lovinger

Contribution from Bell Laboratories, Lucent Technologies, 600 Mountain Ave., Murray Hill, New Jersey 07974

Received August 13, 1997

Abstract: The synthesis, thin-film morphology, and hole mobility in thin-film transistors (TFTs) of compounds based on the novel anthradithiophene (ADT) ring system are reported. The parent compound and its 2,8-dihexyl, didodecyl, and dioctadecyl derivatives (DHADT, DDADT, and DOADT, respectively), synthesized via alkylated thiophene dicarboxaldehyde acetals, were investigated. They all form highly ordered polycrystalline vacuum-evaporated films with mobilities as high as 0.15 $cm^2/(V\ s)$, as high as has ever been observed for a polycrystalline organic material. DOADT has a mobility of 0.06 $cm^2/(V\ s)$ even though 70% of its molecular volume is occupied by hydrocarbon chains. DHADT was cast from solution under atmospheric conditions onto a TFT giving a mobility of 0.01−0.02 $cm^2/(V\ s)$. Thus, the alkylated ADTs combine a pentacene-like intrinsic mobility with greater solubility and oxidative stability.

Thin-film transistors (TFTs), illustrated in Figure 1, are emerging as key devices for a growing worldwide effort to develop organic-based and printed electronic components,[1] an effort that also encompasses light-emitting diodes (LEDs),[2] rectifiers,[3] and capacitors.[4] Applications for TFTs range from display drivers[5] to identification cards and other memory and logic elements.[6] The main technological advantage of organic or "plastic" electronics is the ability to produce useful circuits without the most capital- or labor-intensive steps associated with silicon processing. Secondary advantages are the greater mechanical flexibility and easier tunability of organic devices relative to those fabricated on silicon chips. While it is doubtful that organic materials will rival the inorganics in terms of device performance, they may be useful in applications where device density and reliability under extreme conditions can be sacrificed in favor of ease of processing.

The most important material properties for the semiconductors that comprise the active materials in organic TFTs are high mobility, low "off"-conductivity, stability, and processability. These attributes have been realized to some extent in p-channel (hole-transporting) materials, exemplified by a group of linear, conjugated molecules including thiophene oligomers,[7] a benzodithiophene dimer,[8] and pentacene[9] (Chart 1). Other types of structures that show significant hole-transporting activity in TFTs include phthalocyanines[10] and poly(alkylthiophenes).[11] The oxidation potentials of these compounds are near 1 V vs the standard calomel electrode (SCE), corresponding to a highest occupied molecular orbital (HOMO) energy of about 5 V below vacuum. The electronic energy levels provide for facile hole injection from electrode materials at accessible voltages, while the molecular shape ensures useful mobility by virtue of the intermolecular overlap and molecular orientation in a solid film. For the linear compounds, the mobility appears to increase with the rigidity of the molecule, with pentacene possessing an

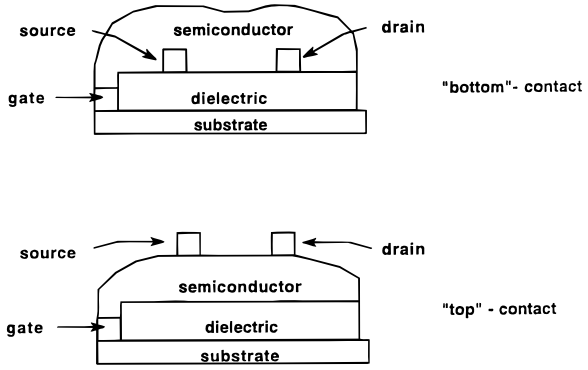

Figure 1. TFT structure showing two different device geometries.

(1) (a) Katz, H. E. *J. Mater. Chem.* **1997**, *7*, 369−376. (b) Garnier, F.; Hajlaoui, R.; Srivastava, P. *Science* **1994**, *265*, 684. (c) Garnier, F. *Pure Appl. Chem* **1996**, *68*, 1455. (d) Bao, Z.; Feng, Y.; Dodabalapur, A.; Raju, V. R.; Lovinger, A. J. *Chem. Mater.* **1997**, *9*, 1299.

(2) Dodabalapur, A. *Solid State Commun.* **1997**, *102*, 259.

(3) Hide, F.; Greenwald, Y.; Wudl, F.; Heeger, A. J. *Synth. Met.* **1997**, *85*, 1255.

(4) Jeon, N. L.; Clem, P. G.; Nuzzo, R. G.; Payne, D. A. *J. Mater. Res.* **1995**, *10*, 2996.

(5) (a) Stubb, H.; Punkka, E.; Paloheimo, J. *Mater. Sci. Eng.* **1993**, *10*, 85. (b) Jarrett, C. P.; Friend, R. H.; Brown, A. R.; de Leeuw, D. M. *J. Appl. Phys.* **1995**, *77*, 6289.

(6) Brown, A. R.; Pomp, A.; Hart, C. M.; de Leeuw, D. M. *Science* **1995**, *270*, 972.

(7) (a) Garnier, F.; Horowitz, G.; Peng, X. Z.; Fichou, D. *Synth. Met.* **1991**, *45*, 163. (b) Servet, B.; Horowitz, G.; Ries, S.; Lagorsse, O.; Alnot, P.; Yassar, A.; Deloffre, F.; Srivastava, P.; Hajlaoui, R.; Lang, P.; Garnier, F. *Chem. Mater.* **1994**, *6*, 1809. (c) Dodabalapur, A.; Torsi, L.; Katz, H. E. *Science* **1995**, *268*, 270.

(8) Laquindanum, J. G.; Katz, H. E.; Lovinger, A. J.; Dodabalapur, A. *Adv. Mater.* **1997**, *9*, 36.

(9) (a) Laquindanum, J. G.; Katz, H. E.; Lovinger, A. J.; Dodabalapur, A. *Chem. Mater.* **1996**, *8*, 2542. (b) Lin, Y. Y.; Gundlach, D. J.; Jackson, T. N. *Annual Device Research Conference Digest, 54th*; IEEE: Santa Barbara, CA, 1996; p 175. See also: *Science* **1996**, *273*, 879. (c) Dimitrakopoulos, C. D.; Brown, A. R.; Pomp, A. J. *J. Appl. Phys.* **1996**, *80*, 2501.

(10) Bao, Z.; Lovinger, A. J.; Dodabalapur, A. *Appl. Phys. Lett.* **1996**, *69*, 3066.

(11) (a) Bao, Z.; Lovinger, A. J.; Dodabalapur, A. *Appl. Phys. Lett.* **1996**, *69*, 4108. (b) Tsumura, A.; Koezuka, H.; Ando, T. *Appl. Phys Lett.* **1986**, *49*, 1210.

S0002-7863(97)02838-2 CCC: $15.00
Published on Web 01/16/1998

Chart 1

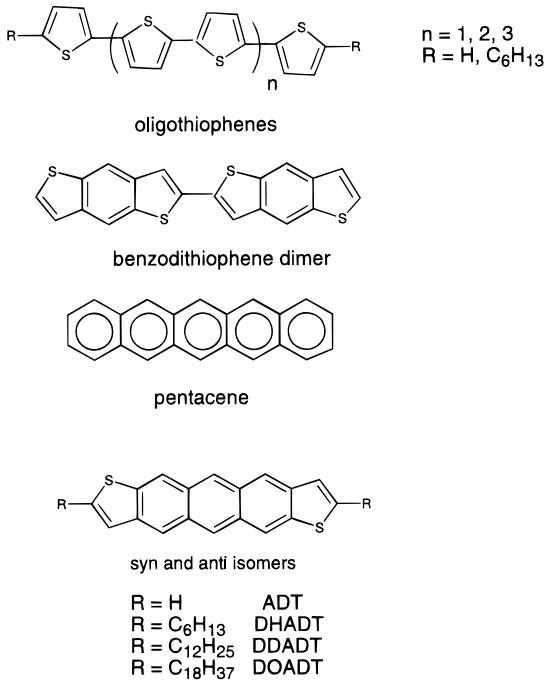

extraordinary TFT mobility of ca. 1 $cm^2/(V\ s)$[12] under deposition conditions that lead to a favorable morphology. Nevertheless, pentacene suffers from the disadvantages of oxidative instability,[13] extreme insolubility, and, for display applications, a strong absorbance throughout the visible spectrum. Where photoinduced decomposition reactions could occur, this absorbance would make pentacene sensitive to most visible light.

The closely related fused heterocycles with the anthradithiophene structure have never been reported, although the dione precursors have been prepared.[14] On the basis of the ring system, anthradithiophene (ADT) would be expected to have a suitable HOMO energy and solid-state structure for use as a p-channel TFT semiconductor. In addition, the barrier to oxidation could be higher than that for pentacene because of the expected greater loss of aromaticity that would accompany oxygen addition across the central ring relative to the pentacene case. Finally, the susceptibility of the C−H bonds α- to the sulfurs at the ends of anthradithiophene presents an avenue for end substitution that is not present in pentacene, so that the solubility, morphology, and adhesion could be better defined.

In this paper, we report the synthesis of the parent compound, ADT, and the end-substituted derivatives dihexyl-, didodecyl-, and dioctadecyl-ADT (DHADT, DDADT, and DOADT, respectively, Chart 1). All of these compounds are obtained and investigated as mixtures of syn and anti isomers. Besides the usual thermal and analytical characterization, we explore the crystallinity and morphology of these compounds as evaporated thin films. Application of these compounds as the semiconductors in TFTs gives devices with some of the highest mobilities ever observed for polycrystalline organic films, even in cases where the film consists predominantly of alkyl groups. We conclude with a brief study of the mobility of DHADT films cast from solution.

(12) (a) Jackson, T. N. Presented at the 1996 Materials Research Society Fall Meeting, Boston, MA, November 1996; paper D6.1. (b) Lin, Y. Y.; Gundlach, D. J.; Nelson, S. F.; Jackson, T. N. *IEEE Transactions on Electronic Devices* **1997**, *44*, 1325.

(13) Yamada, M.; Ikemote, I.; Kuroda, H. *Bull. Chem. Soc Jpn.* **1988**, *61*, 1057.

(14) De la Cruz, P.; Martin, N.; Miguel, F.; Seoane, C.; Albert, A.; Cano, H.; Gonzalez, A.; Pingarron, J. M. *J. Org. Chem.* **1992**, *57*, 6192.

Experimental Section

All starting materials were purchased from Aldrich and were used as received unless otherwise specified. THF was distilled from sodium benzophenone ketyl. NMR spectra were collected with use of a Bruker 360 MHz spectrometer with $CDCl_3$ as solvent and tetramethylsilane (TMS) as an internal standard. Mass spectra were recorded on a Hewlett-Packard 5989A mass spectrometer. Thermal analyses were performed with a Perkin-Elmer DSC 7 analyzer. Elemental analyses were done by Robertson Microlit Laboratories. Molecular modeling was performed with the Spartan version of the AM1 semiempirical method and Cerius system from Molecular Simulations, Inc.

TFT devices composed of ADT and its dialkyl-substituted derivatives were prepared by subliming the materials onto prepared TFT substrates at pressures of 3×10^{-6} Torr or lower, using deposition rates of ca. 5 Å/s. The temperature of the substrates was controlled by heating the copper block on which they were mounted. Two different substrate configurations were used to make the TFT devices, "bottom" and "top" contacts, respectively, illustrated in Figure 1. For both configurations, a silicon dioxide dielectric layer was thermally grown on n-doped silicon which acts as the gate. In the bottom-contact geometry, conduction channels were photolithographically defined with a channel width (W) of 250 μm and channel lengths (L) between 1.5 and 25 μm. The semiconductor was sublimed onto the entire substrate above the dielectric and electrodes. For the top contact geometry, however, the electrodes were defined after sublimation of the semiconductor by using shadow masks of W/L of ca. 1.5/1 and 4/1. The active semiconductor film area for the two values of W/L was ca. $3-4 \times 10^4$ μm^2 and 4 mm^2, respectively. Gold was used as the metal contact for all devices. The electrical characterizations were performed at room temperature under vacuum with use of a 4145b Hewlett-Packard semiconductor parameter analyzer.

For morphological characterizations, the materials were deposited onto carbon-coated electron microscope grids and Si/SiO_2 chips simultaneously with the TFTs. X-ray diffraction studies were done with use of films on the Si/SiO_2 chips in the reflection mode at 40 kV and 25 mA. A 2-kW Rigaku X-ray generator was used as a source of Ni-filtered Cu Kα radiation. The fims on the grids used for electron microscopy were shadowed with Pt/C at $\tan^{-1}$ 1/2 and lightly carbon-coated in a vacuum evaporator before examination with a JEOL transmission microscope operated at 100 kV.

Anthra[2,3-*b*:6,7-*b*′]dithiophene-5,11-dione and Anthra[2,3-*b*:7,6-*b*′]dithiophene-5,11-dione (1). Compound **1** was obtained by following a previously published procedure.[14]

Anthra[2,3-*b*:6,7-*b*′]dithiophene and Anthra[2,3-*b*:7,6-*b*′]dithiophene (2). Aluminum wire (1.0 g) was reacted in 30 mL of dry cyclohexanol containing mercuric chloride (0.02 g) and carbon tetrachloride (0.2 mL) by warming slowly to mild reflux and controlled by cooling. The reaction was completed by refluxing under a nitrogen atmosphere overnight. The dione (1.0 g, 3 mmol) was added and the resulting mixture refluxed under nitrogen for 48 h. The reaction mixture was cooled to 50 °C and centrifuged to collect the solid product. The solids were washed with warm cyclohexanol followed by glacial acetic acid, 10% HCl, and ethanol several times. The crude product was purified by using vacuum sublimation at pressures of 10^{-4} Torr or lower to give a bright orange solid (0.46 g) in 53% yield. Mp = 450 °C Anal. Calcd for $C_{18}H_{10}S_2$: C, 74.45; H, 3.47; S, 22.08. Found: C, 74.23; H, 3.49; S, 22.25. MS (*m*/*e*) 390 (M^+, 100).

2,3-Bis(1,3-dioxolan-2-yl)thiophene (3). 2,3-Thiophene dicarboxaldehyde (2 g, 14 mmol), *p*-toluenesulfonic acid monohydrate (2 mg), and ethylene glycol (1.96 g, 30 mmol) were added to 25 mL of dry benzene. The mixture was refluxed and water was collected in a Dean-Stark trap. After cooling, the reaction mixture was washed with 10% NaOH then H_2O and dried over $MgSO_4$. The product was used directly in the succeeding step without purification. NMR ($CDCl_3$) δ 4.03 (t), 4.11 (t), 6.05 (s), 6.33 (s), 7.11 (d, J = 5.2 Hz), 7.27 (d, J = 5.55 Hz).

2,3-Bis(1,3-dioxolan-2-yl)-5-hexylthiophene (4a). **3** (3 g, 10.3 mmol) was dissolved in 50 mL of dry THF under N_2 and cooled to −78 °C. *n*-BuLi (6.8 mL, 2.5 M in hexane) was added dropwise. After 5 min, 1-iodohexane (2.5 mL, 17 mmol) was added. The solution was stirred at −78 °C and was left to warm to room temperature overnight. Ether (30 mL) was added and the organic layer was washed several times with water. The organic extract was dried over $MgSO_4$ and concentrated. The crude product was purified by column chromatography with use of silica gel (1:2 ethyl acetate:hexane) to give 2.28 g (71%) of **4a** as a yellow oil. NMR ($CDCl_3$) δ 0.85 (t), 1.27−1.4 (m), 1.67 (q), 2.74 (t), 3.93 (t), 4.1 (t), 5.96 (s), 6.26 (s), 6.77 (s).

2,3-Bis(1,3-dioxolan-2-yl)-5-dodecylthiophene (4b). The same procedure as for compound **4a** was used with the following amounts of starting material: **3** (2 g, 9 mmol), *n*-BuLi (4.2 mL, 2.5 M in hexane), and 1-iodododecane (3.12 g, 10.5 mmol). NMR ($CDCl_3$) δ 0.88 (t), 1.2−1.42 (m), 1.65 (q), 2.74 (t), 4.05 (t), 4.13 (t), 5.98 (s), 6.30 (s), 6.79 (s).

2,3-Bis(1,3-dioxolan-2-yl)-5-octadecylthiophene (4c). The same procedure as for compound **4a** was used with the following amounts of starting material: **3** (2 g, 9 mmol), *n*-BuLi (4.2 mL, 2.5 M in hexane), and 1-iodooctadecane (3.84 g, 10 mmol). NMR ($CDCl_3$) δ 0.88 (t), 1.2−1.42 (m), 1.65 (q), 2.74 (t), 4.05 (t), 4.13 (t), 5.98 (s), 6.30 (s), 6.79 (s).

General Procedure for Deprotection of 5-Alkylthiophene Diacetals. A solution of the diacetal-protected compound in 50 mL of THF and 3 N HCl was refluxed for at least 15 min. The solution was cooled to room temperature. Ice was added and the mixture was extracted with ether. The combined organic extract was washed with dilute sodium bicarbonate and dried over $MgSO_4$. The product was used directly without purification.

5-Hexyl-2,3-thiophenedicarboxaldehyde (5a): NMR ($CDCl_3$) δ 0.92 (t), 1.22−1.45 (m), 1.75 (q), 2.9 (t), 7.34 (s), 10.33 (s), 10.41(s).

5-Dodecyl-2,3-thiophenedicarboxaldehyde (5b): NMR ($CDCl_3$) δ 0.9 (t), 1.22−1.45 (m), 1.75 (q), 2.9 (t), 7.35 (s), 10.36 (s), 10.40 (s).

5-Octadecyl-2,3-thiophenedicarboxaldehyde (5c): NMR ($CDCl_3$) δ 0.9 (t), 1.2−1.38 (m), 1.75 (q), 2.85 (t), 7.32 (s), 10.33 (s), 10.4 (s).

2,8-Dihexylanthra[2,3-*b*:6,7-*b*′]dithiophene-5,11-dione and 2,8-Dihexylanthra[2,3-*b*:7,6-*b*′]dithiophene-5,11-dione (6a), 2,8-Didodecylanthra[2,3-*b*:6,7-*b*′]dithiophene-5,11-dione and 2,8-Didodecylanthra[2,3-*b*:7,6-*b*′]dithiophene-5,11-dione (6b), and 2,8-Dioctadecylanthra[2,3-*b*:6,7-*b*′]dithiophene-5,11-dione and 2,8-Dioctadecylanthra[2,3-*b*:7,6-*b*′]dithiophene-5,11-dione (6c). These compounds were synthesized by using a published procedure as for compound **1**. The product in each case was a yellow-green solid (yields: 30−80%) that was used in the next step without purification. No attempt was made to separate the syn and the anti isomers.

2,8-Dihexylanthra[2,3-*b*:6,7-*b*′]dithiophene and 2,8-Dihexylanthra[2,3-*b*:7,6-*b*′]dithiophene (7a). The procedure used was the same as for compound **2** with the following amounts of starting materials: **6a** (0.37 g, 0.7 mmol), as well as Al (0.25 g), $HgCl_2$ (0.005 g), CCl_4 (0.2 mL) in 25 mL of cyclohexanol. The crude product was purified by vacuum sublimation at a pressure of ca. 10^{-4} Torr to give a bright orange solid (0.1 g). Mp = 395 °C. Anal. Calcd for $C_{30}H_{34}S_2$: C, 78.55; H, 7.47; S, 13.98. Found: C, 78.38; H, 7.20; S, 13.69. MS (*m*/*e*) 4580 (M^+, 100), 386 (10%), 316 (20%).

2,8-Didodecylanthra[2,3-*b*:6,7-*b*′]dithiophene and 2,8-Didodecylanthra[2,3-*b*:7,6-*b*′]dithiophene (7b). The procedure used was the same as for compound **2** with the following amounts of starting materials: **6b** (0.9 g, 1.4 mmol), Al (0.4 g), $HgCl_2$ (0.01 g), CCl_4 (0.2 mL) in 50 mL of cyclohexanol. The crude product (0.42 g) was purified by vacuum sublimation at a pressure of ca. 10^{-4} Torr to give a bright orange solid (0.23 g). Mp = 322 °C. Anal. Calcd for $C_{42}H_{58}S_2$: C, 80.45; H, 9.32; S, 10.23. Found: C, 80.33; H, 9.33; S, 10.00.

2,8-Dioctadecylanthra[2,3-*b*:6,7-*b*′]dithiophene and 2,8-Dioctadecylanthra[2,3-*b*:7,6-*b*′]dithiophene (7c). The procedure used was the same as for compound **2** with the following amounts of starting materials: **6c** (0.86 g, 1.0 mmol), Al (0.27 g), $HgCl_2$ (0.006 g), CCl_4 (0.2 mL) in 50 mL of cyclohexanol. The crude product (0.22 g) was purified by vacuum sublimation at a pressure of ca. 10^{-4} Torr to give a bright orange solid (0.14 g). Mp = 270 °C Anal. Calcd for $C_{54}H_{82}S_2$: C, 81.55; H, 10.39; S, 8.06. Found: C, 81.39; H, 10.17; S, 7.99.

Scheme 1

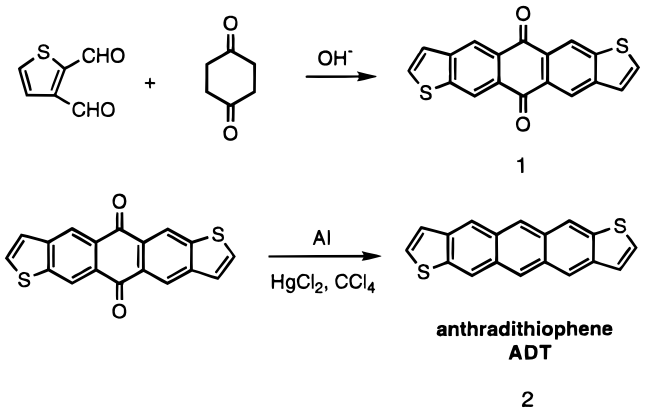

Results

Synthesis. Anthradithiophene (**2**) was synthesized according to Scheme 1. (As already mentioned, all the fused ring compounds pictured in the schemes, though drawn as anti isomers, are prepared as syn−anti isomeric mixtures.) The synthesis is a two-step procedure wherein the first step involves a cyclization reaction to form the dione. The synthesis of the dione was based on a published procedure,[14] starting with commercially available 2,3-thiophene dialdehyde reacting with 1,4-cyclohexanedione under basic conditions. The resulting dione (**1**) was reduced by using a procedure similar to that used to synthesize pentacene.[15] The reducing agent was $Al(OCy)_3$, which was formed in situ by letting aluminum strips react in a mixture of mercuric chloride and carbon tetrachloride in anhydrous cyclohexanol. The dialkyl-substitued derivatives of ADT were synthesized according to Scheme 2. The synthesis involved the protection of thiophene dialdehyde as a bis-acetal, which is stable to basic conditions. The alkylation reaction was done by lithiating the diacetal-protected thiophene at the 2-position and then reacting with an alkyl halide. Three different alkyl chains were used in this study, hexyl (**4a**), dodecyl (**4b**), and octadecyl (**4c**). After the alkyl groups have been attached to the thiophene ring, the acetal protecting groups were removed by refluxing the material in acid to obtain the alkylated dialdehydes **5a**, **5b**, and **5c**. These materials were then allowed to react with 1,4-cyclohexanedione in a manner similar to the synthesis of the unsubstituted ADT to obtain the novel compounds DHADT (**7a**), DDADT (**7b**), and DOADT (**7c**).

Thermal analyses of ADT, DHADT, DDADT, and DOADT showed melting points decreasing with chain length. The solubilities of the dialkylated compounds were also tested in toluene and chlorobenzene. All of the materials were shown to be soluble in refluxing toluene (0.5 mg/mL) and chlorobenzene (2 mg/mL) with DHADT showing some slight solubility in room temperature toluene.

To assess the stability of dissolved ADT compounds, a sample of DHADT was dissolved in 1,2-dichlorobenzene under ambient light and atmosphere. No change in color was observed in a saturated solution over hours at room temperature. Recrystallized material recovered from the solution melted at 395 °C, identical with the original solid. This is in contrast to pentacene,

(15) Goodings, E. P.; Mitchard, D. A.; Owen, G. *J. Chem. Soc., Perkin Trans. 1* **1972**, *11*, 1310.

Scheme 2

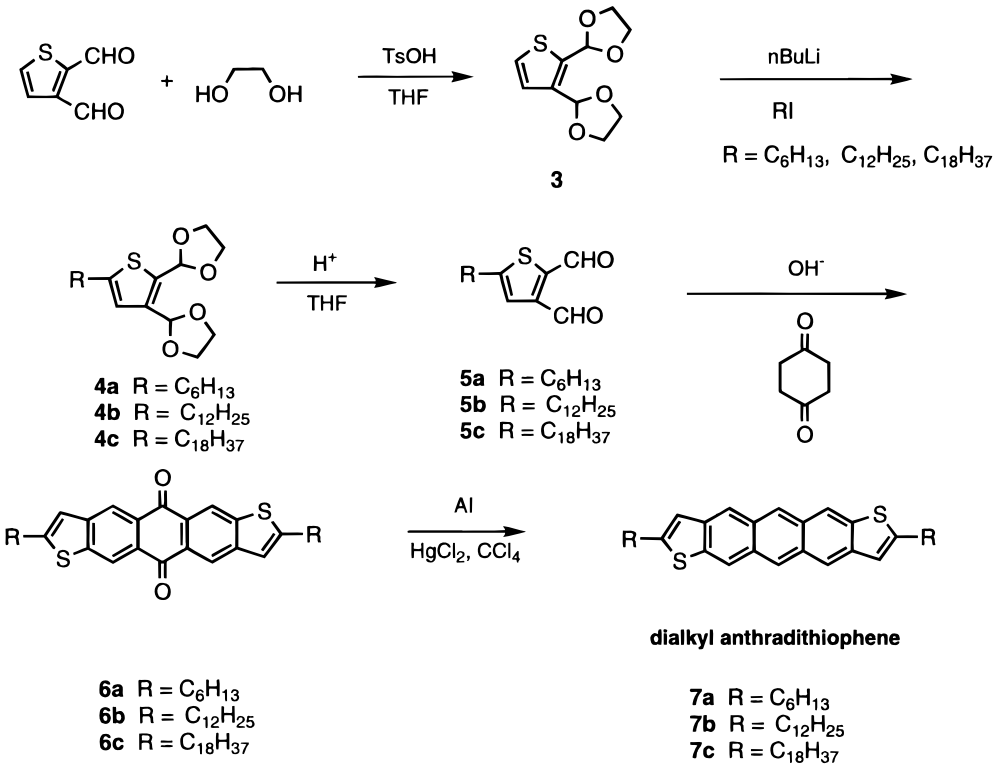

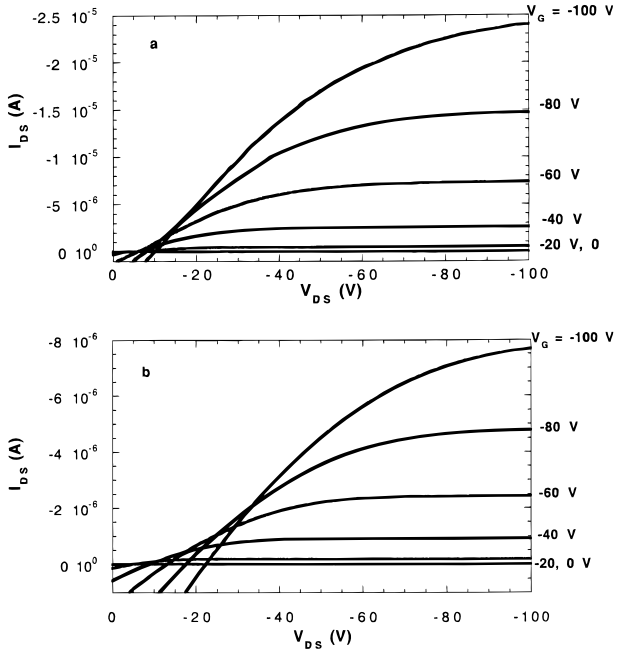

Figure 2. Source-drain current vs voltage (I_{DS} vs V_{DS}) characteristics of a DHADT TFT with (a) *W*/*L* of 250/12 ("bottom"-contact geometry) and (b) *W*/*L* ca. 1.5/1 ("top"-contact geometry) at different gate voltages deposited at T_{sub} = RT. The increasing deviations from zero current at zero drain-source voltage with higher gate voltages are caused by leakage through the dielectric.

which is virtually insoluble. The small quantity of pentacene that could be extracted into refluxing 1,2-dichlorobenzene bleached in less than 5 min.

Electrical Characteristics. The field-effect mobilities (μ_{FET}) of the TFT devices with ADT and its dialkylated derivatives were determined by using two different device geometries, namely "top", and "bottom"-contact geometries. In the former case, the semiconductor is deposited first and electrodes are then defined by using a shadow mask. Two different types of channel width (*W*) to length (*L*) ratios were used in the "top"-contact experiments, *W*/*L* of ca. 1.5/1 and 4/1. For the "bottom"-contact geometry, sources and drains are photolithographically defined and the deposition of the semiconductor material is the final step to complete the device. For all of the devices, the mobilities were determined in the saturation regime ($V_{DS} > V_{GS}$) by using the equation[16]

$$I_{DS} = \frac{WC_i}{2L}\mu(V_G - V_o)^2 \qquad (1)$$

where *C*, the insulator capacitance, is 10 nF/cm^2 and V_o is the extrapolated threshold voltage. The materials showed an enhancement in the current at negative gate-souce voltages (V_{GS}s), which indicates that the materials transport holes and are, therefore, p-channel materials. An example of an *I*−*V* curve is shown in Figure 2.

Table 1. Field-Effect Mobilities of ADT as a Function of Substrate Deposition Temperature

temp (°C)	mobility (cm^2/V s)
RT	0.02
60	0.04
70	0.03−0.06
85	0.09
100	no FET behavior

The mobilities of ADT with "bottom"-contact device geometry at different substrate deposition temperatures, T_{sub}, are listed in Table 1. The mobility was shown to increase with increasing temperature with the highest mobility of 0.09 cm^2/(V s) achieved at T_{sub} = 85 °C. At temperatures above T_{sub} = 85 °C, FET activity was not observed.

The mobilities of dialkyl-substituted derivatives are listed in Table 2. From the table, mobilities of >0.1 cm^2/(V s) were

(16) Torsi, L.; Dodabalapur, A.; Katz, H. E. *J. Appl. Phys.* **1995**, *78*, 1088.

Table 2. Structural and Electrical Characteristics of Alkylated ADTs as a Function of Substrate Deposition Temperatures

material	temp (°C)	repeat spacing (nm)	morphology	mobility (cm^2/V s)
DHADT	RT	2.55	smooth, interconnected grains	0.11 ± 0.01
	85	2.6	smooth, interconnected grains	0.15 ± 0.02
	125	2.62	smooth, interconnected grains	0.12 ± 0.02
DDADT	RT	3.83	elongated, interconnected grains	0.12 ± 0.02
	85	peak not resolvable	elongated, interconnected grains	0.14 ± 0.02
	125	3.68	flat, smooth	0.04 ± 0.01
DOADT	RT	peak not resolvable	small, elongated grains	0.06 ± 0.01
	85	peak not resolvable	large, elongated grains	0.06 ± 0.01
	125	4.64	flat, extended lamellae	0.04 ± 0.001

achieved, comparable to the highest mobilities reported for polycrystalline organic p-channel materials. The mobilities of the dialkyl-substituted ADT derivatives were also determined at different substrate temperatures. For this set of compounds, "top"-contact geometries of *W*/*L* ca. 1.5/1 were used since the mobilities calculated with "bottom"-contact geomteries were irreproducible and were scattered over a wide range of values. Similar to ADT, the mobilities of the dialkylated derivatives show a dependence on the substrate deposition temperatures. The dependence on the deposition temperatures is most apparent for DDADT, wherein there was an order of magnitude drop in the mobilities as the substrate deposition temperature was increased from 85 to 125 °C. The electrical characteristics of DHADT with use of "top"-contact geometries with channel dimensions of *W*/*L* of 4/1 gave mobilities 30% lower than those achieved by using smaller channel dimensions. This could be due to the larger quantity of heat produced in depositing the larger pads for *W*/*L* of 4/1, or the greater probability of finding a particularly severe defect in the larger active region.

TFT devices using DHADT cast from solution were also prepared and their mobilities calculated. Dilute solutions (ca. 0.2−1%) of DHADT in hot chlorobenzene were prepared and cast onto prepared TFT "bottom"-contact substrates. The solvent was then left to evaporate in a vacuum oven with different oven temperatures. No field-effect activity was observed when the solutions were evaporated at room temperature and 50, 150, and 180 °C. However, FET activity was observed when the solutions were evaporated at oven temperatures of 70 and 100 °C. Field-effect mobilities of 6×10^{-4} to 3×10^{-3} cm^2/(V s) were calculated for devices prepared at 70 °C while those prepared at 100 °C gave mobilities in the 0.01−0.02 cm^2/(V s) range.

Morphology. X-ray diffraction studies of ADT films deposited at different substrate temperatures indicate an exceptionally high degree of ordering with very sharp reflections at 1.415, 0.710, 0.470, and 0.356 nm (see Figure 3). The first of these corresponds exactly to the length of the ADT molecule and the others are its second, third, and fourth orders, respectively. These results demonstrate that the ADT molecules are deposited with exceptionally high order and crystallinity in a perpendicular orientation with respect to their substrates. The same structure, high order, and perpendicular orientation were also found for the samples deposited at the higher temperatures.

The morphologies of ADT deposited at room temperature, 85 °C, and 100 °C are shown in Figure 4 with their corresponding electron-diffraction patterns. The three strongest reflections are at 0.443, 0.360, and 0.301 nm, repectively. Their absence in Figure 3 (as well as the total absence of the very intense peaks from Figure 3 in the electron-diffraction pattern) confirms the perpendicular orientation of the ADT molecules on the substrates. As temperature is increased, there is a corresponding

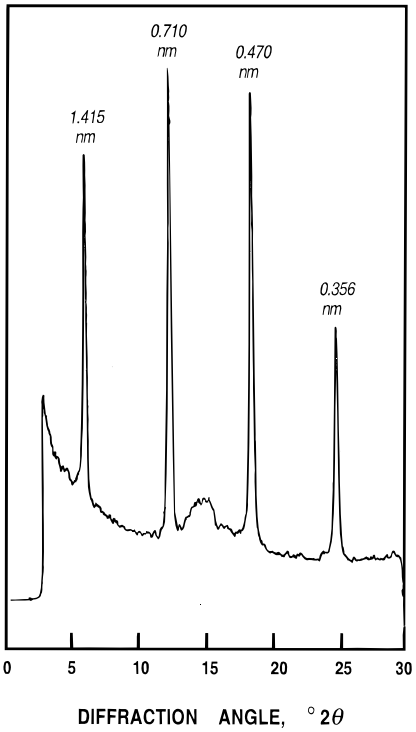

Figure 3. X-ray diffractogram of ADT films on Si/SiO_2, deposited by sublimation at room temperature.

increase in the crystallite sizes from <100 nm at 25 °C to ca. 200 nm at 85 °C. This could explain the higher mobilities obtained at 85 °C compared to room temperature. The absence of any FET activity at $T_{sub} = 100$ °C can be attributed to the formation of large (ca. 400 nm) but widely separated crystals instead of interconnected crystalline grains. Mobility as a function of substrate temperature depends on a tradeoff among factors that enhance mobility, such as chemical and morphological homogeneity and domain continuity, all of which are improved at higher substrate temperature, and interdomain spacing and intracrystallite fracturing, which also increase at higher substrate temperatures (or upon cooling therefrom) and which severely diminish mobiity.

The morphology of the dialkyl-substituted ADT derivatives was studied at three different substrate temperatures, room temperature, 85 °C, and 125 °C. The electron diffraction patterns of DHADT films at the three temperatures demonstrate very high crystallinity and orientation in the same manner as ADT and α6T,[14b,17] i.e., with the long axis nearly perpendicular to the substrate. The X-ray patterns at all substrate temperatures show an extremely sharp and strong peak at 2θ of 3.35° (d = ca. 2.6 nm), which is in excellent agreement with the molecular

(17) Lovinger, A. J.; Davis, D. D.; Ruel, R.; Torsi, L.; Dodabalapur, A.; Katz, H. E. *J. Mater. Res.* **1995**, *10*, 2958.

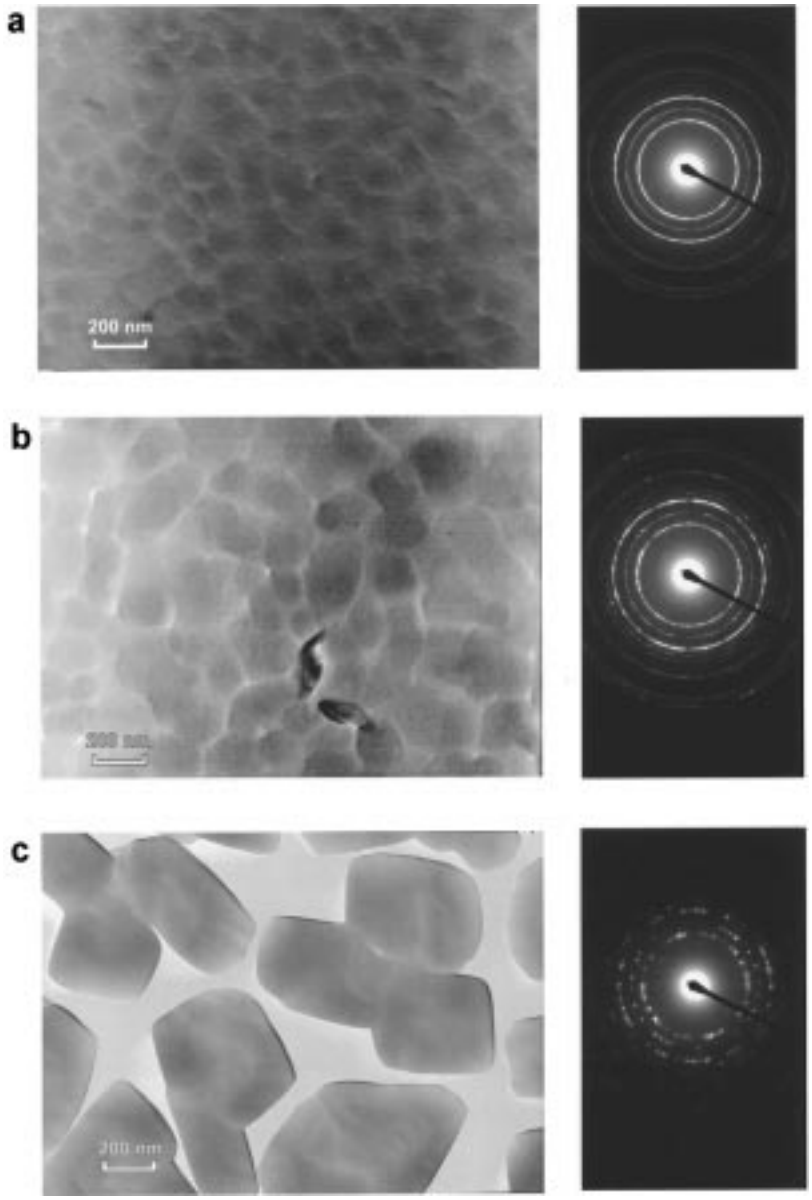

Figure 4. Transmission electron micrographs and selected-area diffraction patterns of ADT films deposited at T_{sub} = RT (a), 85 °C (b), and 100 °C (c).

length of DHADT. The basic morphology consists of nodular nanocrystals, which are no larger than ca. 20 nm even at the higher substrate temperatures; in corresponding electron-diffraction patterns, the strongest reflections are at 0.477 and 0.295 nm, arising from the interchain packing of the molecules on edge.

The DDADT film morphologies for RT and 85 °C consist of elongated, three-dimensional grains ca. 20 × 100 nm. At 125 °C, however, the morphology becomes flat and featureless; this change may be related to the drop in mobility. As for DHADT, DDADT also shows very sharp electron-diffraction rings at all temperatures, implying very high crystallinity. Their spacings are the same as we found for DHADT, which indicates that the interchain packing of these long, alkyl-substituted ADT molecules is the same. At all temperatures studied, X-ray diffraction in the reflection mode showed an edge-on orientation, although in most cases only the first-order peak was seen. However, for DDADT films deposited at 125 °C, the X-ray diffraction pattern is composed of six orders of the main molecular repeat at 2θ of 2.40 ° (d = 3.68 nm). This repeat spacing, however, is somewhat less than the molecular length of DDADT (4.0−4.3 nm depending on conformation), which indicates that the chains are slightly inclined or interdigitated.

X-ray diffraction studies of DOADT films deposited at RT and 85 °C show no resolvable peaks at low angles, which is expected from the findings from DDADT. In this case, excellent ordering is even less likely because of the greater length of the molecule. The fact that no interchain peaks are seen at higher angles suggests that there is again a unique orientation of the molecules, i.e. close to perpendicular to the substrate. The poor crystallinity deduced from the X-ray diffractograms is confirmed by electron diffraction in the orthogonal direction, which yields a diffuse ring at ca. 0.46 nm for specimens deposited at RT. However, for those deposited at 85 °C, a sharper peak is seen at 0.475 nm, signifying higher crystallinity and edge-on molecular orientation.

Although the underlying structure is still the same as in DHADT and DDADT, the morphologies at these two substrate temperatures are much more three-dimensional and rough (see Figure 5). At RT, the crystallites are poorly defined rodlike grains ca. 20 × 50 nm. At 85 °C, they are much better defined with dimensions ca. 30 × 120 nm, as expected by their growth

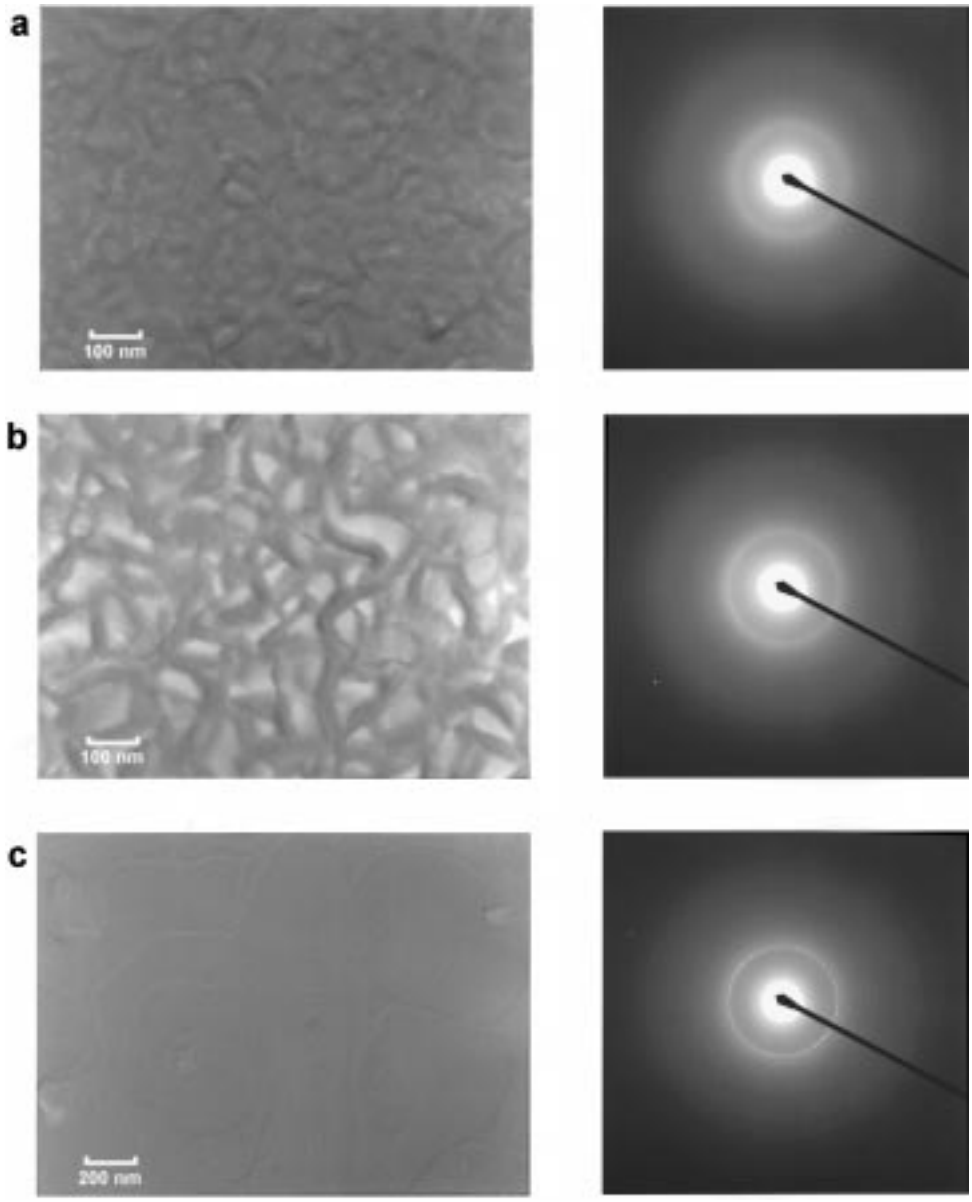

Figure 5. Transmission electron micrographs and selected-area diffraction patterns of DOADT films deposited at T_{sub} = RT (a), 85 °C (b), and 125 °C (c).

at a higher temperature. This trend increases with substrate temperature. Films deposited at 125 °C show very high crystallinity and excellent orientation, with a thin lamellar morphology similar to what is observed in polyethylene films. Terraces and screw dislocations are seen in these films, entirely analogous to what one expects of hydrocarbon chains during slow growth. These morphological features, seen for the first time among the many organic semiconductors studied, reflect the major influence of the long hydrocarbon tails in dictating molecular packing and crystallization in DOADT.

The X-ray diffractogram of DOADT deposited at 125 °C is seen in Figure 6 and depicts exceptionally high order: more than 10 orders of the main molecular repeat at 1.9° 2θ (d = 4.65 nm) are discernible (the first order is actually under the main beam). This is less than the length of an extended planar molecule of DOADT (Figure 7). Molecular modeling suggests that some significant molecular inclination is required to provide the observed d spacing. This might be with the ADT core perpendicular to the substrate (as indicated by the anti isomer at the left of Figure 7) or by some highly inclined (35−40°) orientation.

Discussion

The ring formation and reduction steps that led to ADT and the dialkyl derivatives are analogous to those reported for ADT dione[14] and pentacene,[15] respectively. The new preparative work reported here concerns the method for attachment of the alkyl groups. This was done by protecting the dialdehyde presursor with a group stable to lithiation and alkylation of the 5-carbon. The alkylation step would be generalizable to a wide variety of side chains, including those with some polar functionality,[18] provided the functional groups could withstand the ring closing and reduction reactions. Alternatively, chloroalkyl groups could be introduced, which, given the finite solubility of the alkyl derivatives, could be replaced with nucleophiles at a later stage of the synthetic sequence. While polar side chain functionalization has been accomplished in the case of the thiophene oligomers,[18] the fused ring systems studied until now are not amenable to end substitution. Side groups

(18) (a) Katz, H. E.; Laquindanum, J. G.; Lovinger, A. J. *Chem. Mater.* **1998**, accepted for publication. (b) Wei, Y.; Yang, Y.; Yeh, J.-M. *Chem. Mater.* **1996**, *8*, 2659.

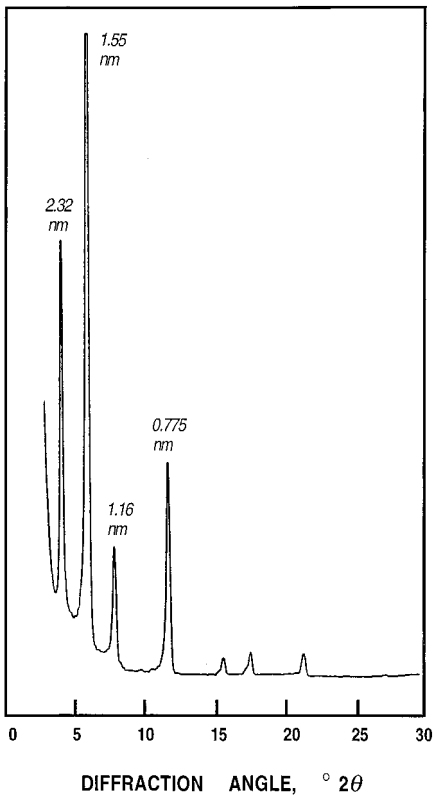

Figure 6. X-ray diffractogram of DOADT films on Si/SiO_2, deposited by sublimation at 125 °C.

could be useful in optimizing the self-assembly, processability, and/or adhesion of the semiconducting films.

The stability of the ADTs, as exemplified by DHADT in solution under ambient conditions, is significantly greater than that of pentacene. This is consistent with a molecular modeling study, which showed that the gas-phase conversion of pentacene to its bridged dioxygen adduct is more exothermic than the analogous transformation of ADT.

The morphology and solid-state structures of the ADTs resemble those of the thiophene oligomers in many ways.[7b,17] The compounds pack in layers, with their long axes nearly perpendicular to the planes of the films. This packing motif has been shown to be favorable for high field-effect mobility in a TFT, since the two directions of π overlap coincide with the plane in which the "on" current must flow. The repeat spacings are consistent with reasonable models of the molecular structures, except in the case of very long alkyl chains at high substrate temperatures where the shorter than expected spacings indicate substantial tilting. We see no evidence of isomer segregation or other manifestations of the dual isomer composition of the ADT compounds in the X-ray diffraction patterns. Molecular models indicate that the S and 3-CH groups differ only slightly in their electron density and van der Waals radii, so the two isomers are fairly isostructural. The repeat spacing of DOADT is one of the longest reported for a molecular solid.[19] The observation of a high TFT mobility for this compound is remarkable, in *that the volume of each molecular layer that can transport charge is only ca. 30% and is sandwiched between insulating layers of polyethylene-like chains*. DOADT thus provides the most dramatic demonstration to date of the two-dimensional transport in organic TFTs. The mobility of DOADT is significantly higher than that of regioregular poly-

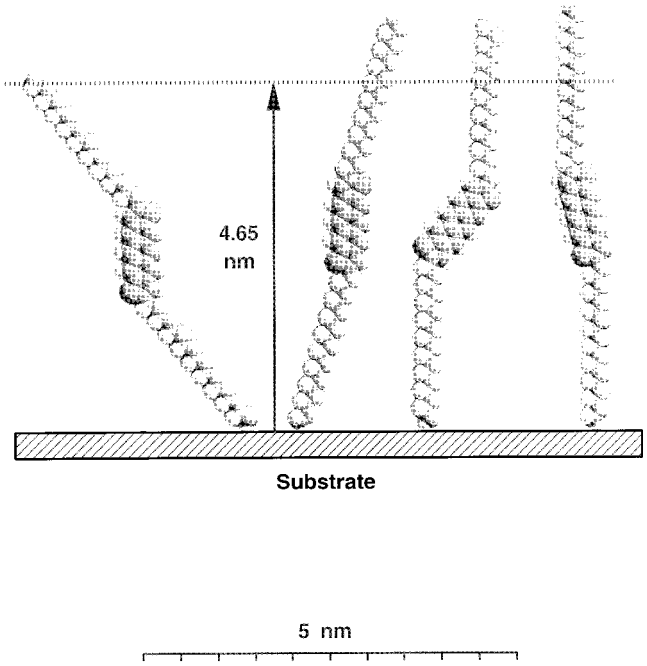

Figure 7. Molecular models of different DOADT conformations and hypothetical substrate arrangements.

(3-octylthiophene),[23] which contains a greater volume fraction of charge transporting material and requires the self-assembly of fewer molecular units. As a second comparison, regioregular poly(3-dodecylthiophene) has a very low mobility.[23] The lack of a strong correlation between structure and mobility in the ADT series emphasizes that it is the planes of fused rings that are solely responsible for the mobility, and suggests that further alterations of the side chains, such as heteroatom substitution, would be possible.

The observed mobilities are consistent with predictions that mobility should increase with increasing rigidity and symmetry along the series of long, conjugated molecules, from α6T to pentacene. However, it should be borne in mind that the high mobility of pentacene is achieved because it forms a single crystal-like film over device dimensions under certain deposition conditions.[9a] Comparing only polycrystalline films, the mobilities of dialkyl ADTs are as high as that of pentacene. If substituents and/or deposition conditions are discovered that lead to formation of a single-crystal film, the mobilities could increase by an order of magnitude. It is also notable that the high mobility is achieved in compounds whose visible absorbance energies (indicative of the "bandgaps") are not particularly low compared to the larger thiophene oligomers and pentacene.

The measured mobilities and on/off ratios reported here are limited by certain experimental factors. Because of the small amounts of material prepared, none of the compounds have been subjected to the slow, ultrahigh vacuum sublimation that removes the last traces of impurities that are probably responsible for the "off" current.[20] The unpatterned nature of the semiconducting film in the TFTs introduces extraneous conduction and leakage paths around the devices being studied, and appears to cause the testing of one device to influence others

(19) Fichou, D.; Bachet, B.; Demanze, F.; Billy, I.; Horowitz, G.; Garnier, F. *Adv. Mater.* **1996**, *8*, 500.

(20) Katz, H. E.; Torsi, L.; Dodabalapur, A. *Chem. Mater.* **1995**, *7*, 2235.

(21) Torsi. L.; Dodabalapur, A.; Lovinger, A. J.; Katz, H. E.; Ruel, R.; Davis, D. D.; Baldwin, K. W. *Chem. Mater.* **1995**, *7*, 2247.

(22) Brown, A. R.; Pomp, A.; de Leeuw, D. M.; Klaasen, D. B. M.; Havinga, E. E.; Herwig, P.; Mullen, K. *J. Appl. Phys.* **1996**, *79*, 2136.

(23) Bao, Z.; Feng, Y.; Dodabalapur, A.; Raju, V. R.; Lovinger, A. J. *Chem Mater.* **1997**, *6*, 1299.

on the same substrate. The fact that most favorable morphologies are obtained at temperatures above 70 °C, where the combined interconnectedness and order in the film appears optimal, means that a cooling process must occur after deposition and before testing. Because of the mismatch in coefficients of thermal expansion between the silicon substrates and the organic films, microcracks[21] can develop which would create barriers to charge transport and lower the apparent mobility. Since most of the channel current flows in the first two monolayers of material,[16] such mobility-lowering defects might be masked by overgrowths and not be readily visible. Moreover, the series resistance in going through the thick polyethylene-like layers to inject charge from top contacts to the channel may be a mobility-lowering factor that is particularly pronounced in DOADT. This may also contribute to the lower mobility of DDADT deposited at 125 °C, even though films deposited at those temperatures are flat, smooth, and highly crystalline. The use of diffraction methods in characterizing these films is subject to the limitation that the important charge-carrying region in the TFT is confined to a few molecular layers near the interface with the dielectric, where the morphology might differ from that of the bulk of the sample that gives rise to most of the diffraction signal.

Taking advantage of the greater solubility and solution stability of the ADTs relative to that of pentacene, it was possible to attempt solution-phase deposition of an ADT derivative, specifically DHADT, as a TFT semiconductor. While the morphologies are clearly inferior and the mobilities lower than for vapor-deposited films, this is the first time such a rigid, high-melting molecule has been found to be processable in this manner without resorting to a precursor route.[1b,22] It is surprising that the best results were obtained from dilute solutions deposited at mildly elevated temperatures, rather than from the more concentrated solutions available at higher temperatures. This may be because in the absence of single-crystal morphology, the multiple nucleation that occurs during growth leads to a more even distribution of the material than at high temperature especially in the first few monolayers. The coefficient of thermal expansion, as discussed above, may also play a role in favoring a lower deposition temperature for significant mobility. The packing of DHADT films deposited from solution may be denser than the film obtained from precursor pentacene, which originates as a highly disordered material. This density increase could in turn lead to greater oxidative stability of the film.

In summary, the fully conjugated, nonoxidized ADT ring system has been synthesized for the first time and the thin film morphology and hole mobility of the parent and three dialkyl derivatives have been explored. In most cases, films deposited by vacuum evaporation are highly crystalline, and the mobilities are among the highest observed in TFT configurations, especially for polycrystalline films. Although on balance the performance of these materials has not proven to be superior to that of pentacene, the ADTs offer advantages in the areas of solubility, processability, and tunability through end-group modification. The results also demonstrate that the high mobility observed for pentacene is not unique among thin films of molecular solids, but may be observable in a wider variety of compounds, including some with lower melting points and larger HOMO−LUMO gaps.

Acknowledgment. The authors wish to thank our colleagues Ananth Dodabalapur, for his help in interpreting some of the results; Zhenan Bao, for valuable discussions; A. M. Mujsce, for obtaining mass spectral analyses, and K. Raghavachari, for his advice on MO calculations.

JA9728381